7. Wootters, W. K. & Zurek, W. H. A single quantum cannot be cloned. *Nature* **299,** 802–803 (1982).
8. Nielsen, M. A. & Chuang, I. J. *Quantum Computation and Quantum Information* (Cambridge Univ. Press, Cambridge, 2000).
9. Gottesman, D. & Chuang, I. L. Demonstrating the viability of universal quantum computation using teleportation and single-qubit operations. *Nature* **402,** 390–393 (1999).
10. Furusawa, A. *et al.* Unconditional quantum teleportation. *Science* **282,** 706–709 (1998).
11. Nielsen, M. A., Knill, E. & Laflamme, R. Complete quantum teleportation using nuclear magnetic resonance. *Nature* **396,** 52–55 (1998).
12. Barrett, M. D. *et al.* Quantum teleportation with atomic qubits. *Nature* (this issue).
13. Schmidt-Kaler, F. *et al.* How to realize a universal quantum gate with trapped ions. *Appl. Phys. B* **77,** 789–796 (2003).
14. Roos, C. F. *et al.* Bell states of atoms with ultra long lifetimes and their tomographic state analysis. *Phys. Rev. Lett.* (in the press) Preprint at ⟨http://arXiv.org/abs/ physics/0307210⟩ (2003).
15. Massar, S. & Popescu, S. Optimal extraction of information from finite quantum ensembles. *Phys. Rev. Lett.* **74,** 1259–1263 (1995).
16. Gisin, N. Nonlocality criteria for quantum teleportation. *Phys. Lett. A* **210,** 157–159 (1996).
17. Kielpinski, D., Monroe, C. & Wineland, D. J. Architecture for a large-scale ion-trap quantum computer. *Nature* **417,** 709–711 (2002).
18. Gulde, S. *et al.* Implementation of the Deutsch-Jozsa algorithm on an ion-trap quantum computer. *Nature* **412,** 48–50 (2003).
19. Hahn, E. L. Spin Echoes. *Phys. Rev.* **80,** 580–594 (1950).

Acknowledgements We thank H. Briegel and P. Zoller for a critical reading of the manuscript. We gratefully acknowledge support by the Austrian Science Fund (FWF), by the European Commission (QUEST, QUBITS and QGATES networks), by the Institut für Quanteninformation, and by the Los Alamos LDRD Program. This material is based upon work supported in part by the US Army Research Office. H.H is funded by the Marie-Curie program of the European Union.

Competing interests statement The authors declare that they have no competing financial interests.

Correspondence and requests for materials should be addressed to R.B. (Rainer.Blatt@uibk.ac.at)

Deterministic quantum teleportation of atomic qubits

M. D. Barrett[1]*, J. Chiaverini[1], T. Schaetz[1], J. Britton[1], W. M. Itano[1], J. D. Jost[1], E. Knill[2], C. Langer[1], D. Leibfried[1], R. Ozeri[1] & D. J. Wineland[1]

[1]*Time and Frequency Division, NIST, Boulder, Colorado 80305, USA*
[2]*Mathematical and Computational Sciences Division, NIST, Boulder, Colorado 80305, USA*

* Present address: Department of Physics, University of Otago, PO Box 56, Dunedin, New Zealand

Quantum teleportation[1] provides a means to transport quantum information efficiently from one location to another, without the physical transfer of the associated quantum-information carrier. This is achieved by using the non-local correlations of previously distributed, entangled quantum bits (qubits). Teleportation is expected to play an integral role in quantum communication[2] and quantum computation[3]. Previous experimental demonstrations have been implemented with optical systems that used both discrete and continuous variables[4–9], and with liquid-state nuclear magnetic resonance[10]. Here we report unconditional teleportation[5] of massive particle qubits using atomic ($^9Be^+$) ions confined in a segmented ion trap, which aids individual qubit addressing. We achieve an average fidelity of 78 per cent, which exceeds the fidelity of any protocol that does not use entanglement[11]. This demonstration is also important because it incorporates most of the techniques necessary for scalable quantum information processing in an ion-trap system[12,13].

Quantum teleportation[1] provides a means for transporting a quantum state between two separated parties, Alice and Bob, through the transmission of a relatively small amount of classical information. For the case of a two-state quantum system or 'qubit', only two bits of classical information are needed, which seems surprising as precise specification of a general qubit state requires an infinite amount of classical information. Aside from the obvious differences in the various experimental demonstrations, the basic teleportation protocol is the same[1]. Alice is in possession of a qubit (here labelled 2) that is in an unknown state $|\psi\rangle_2 \equiv \alpha|\uparrow\rangle_2 + \beta|\downarrow\rangle_2$, where $|\downarrow\rangle$ and $|\uparrow\rangle$ denote eigenstates of the qubit in the measurement basis. In addition, Alice and Bob each possess one qubit of a two-qubit entangled pair that we take to be a singlet $|S\rangle_{1,3} \equiv |\uparrow\rangle_1|\downarrow\rangle_3 - |\downarrow\rangle_1|\uparrow\rangle_3$ (where, for simplicity, we omit normalization factors). Therefore, Alice possesses qubits 1 and 2, while Bob holds qubit 3. Alice wishes to transmit the state of qubit 2 to Bob's qubit using only classical communication. The initial joint state of all three qubits is

$$|\Phi\rangle = |S\rangle_{1,3} \otimes |\psi\rangle_2. \quad (1)$$

This state can be rewritten using an orthonormal basis of Bell states[14] $|\Psi_k\rangle_{1,2} (k = 1–4)$ for the first two qubits and unitary transformations U_k acting on $|\psi\rangle_3 (= \alpha|\uparrow\rangle_3 + \beta|\downarrow\rangle_3)$ so that $|\Phi\rangle = \Sigma_{k=1}^{4} |\Psi_k\rangle_{1,2} (U_k|\psi\rangle_3)$. A measurement in the Bell-state basis $\{|\Psi_k\rangle\}$ by Alice then leaves Bob with one of the four possibilities $U_k|\psi\rangle_3$. Once Bob learns of Alice's measurement outcome (through classical communication), he can recover the original unknown state by applying the appropriate unitary operator, U_k^{-1}, to his state $U_k|\psi\rangle_3$. We note that Alice's Bell-state measurement can be accomplished by transforming from the basis $\{|\Psi_k\rangle_{1,2}\}$ into the measurement basis $\{|\uparrow\uparrow\rangle_{1,2}, |\uparrow\downarrow\rangle_{1,2}, |\downarrow\uparrow\rangle_{1,2}, |\downarrow\downarrow\rangle_{1,2}\}$ before the measurement.

Our implementation uses atomic qubits ($^9Be^+$ ions) that are confined in a linear radiofrequency Paul trap similar to that used in ref. 15. The control electrodes are segmented into eight sections as shown schematically in Fig. 1, providing a total of six trapping zones (centred on electrode segments 2 to 7). Potentials applied to these electrodes can be varied in time to separate ions and move them to different locations. The qubits are composed of the ground-state hyperfine levels $|\uparrow\rangle \equiv |F = 1, m = -1\rangle$ and $|\downarrow\rangle \equiv |F = 2, m = -2\rangle$, which are separated by $\omega_0 \cong 2\pi \times 1.25\,\mathrm{GHz}$. These states are coupled through stimulated Raman transitions[16–18] from two laser

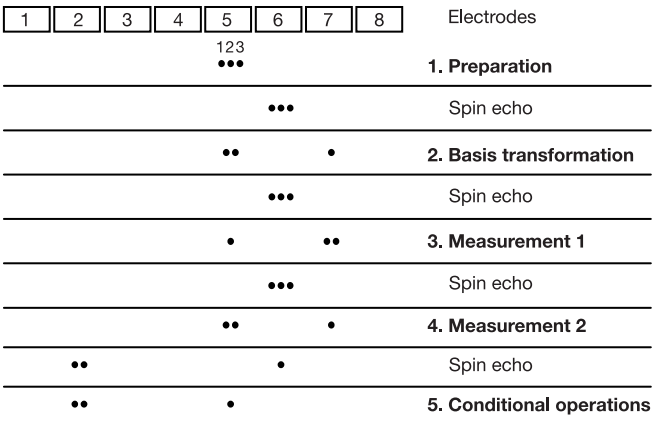

Figure 1 Schematic representation of the teleportation protocol. The ions are numbered left to right, as indicated at the top, and retain their order throughout. Positions, relative to the electrodes, are shown at each step in the protocol. The widths of the electrodes vary, with the width of the separation electrode (6) being the smallest at 100 μm. The spacing between ions in the same trap is about 3 μm, and laser-beam spot sizes (in traps 5 and 6) at the position of the ions are approximately 30 μm. In step 1 we prepare the outer ions in an entangled (singlet) state and the middle ion in an arbitrary state (equation (1)). Steps 2–4 constitute a measurement in a Bell-basis for ions 1 and 2 (Alice's qubits), teleporting the state of ion 2 onto ion 3 (Bob's qubit), up to unitary operations that depend on the measurement outcomes. In step 5 we invoke these conditional operations, recovering the initial state. Interspersed are spin-echo pulses applied in trap 6 that protect the state from de-phasing due to fluctuating magnetic fields but do not affect the teleportation protocol.

beams, which are used to implement the single-qubit rotations

$$R(\theta,\phi) = \cos(\theta/2)I + i\sin(\theta/2)\cos(\phi)\sigma_x + i\sin(\theta/2)\sin(\phi)\sigma_y, \quad (2)$$

where I is the identity operator, σ_x, σ_y and σ_z denote the Pauli spin matrices in the $\{|\uparrow\rangle, |\downarrow\rangle\}$ basis ($\langle\uparrow| \equiv (1,0)$, $\langle\downarrow| \equiv (0,1)$), θ is proportional to the duration of the Raman pulse, and ϕ is the relative phase between the Raman beams at the position of the ion. The Raman beams are also used to generate entanglement between two qubits by implementing the phase gate[18]

$$a|\uparrow\uparrow\rangle + b|\uparrow\downarrow\rangle + c|\downarrow\uparrow\rangle + d|\downarrow\downarrow\rangle \rightarrow a|\uparrow\uparrow\rangle - ib|\uparrow\downarrow\rangle - ic|\downarrow\uparrow\rangle + d|\downarrow\downarrow\rangle. \quad (3)$$

Our teleportation scheme is shown schematically in Fig. 1. We highlight the key elements of the protocol in bold lettering and also include the auxiliary 'spin-echo' pulses[15,18] ($R(\pi,\phi_{SE})$) applied to ions in trap 6. These pulses are required in the experiment to prevent dephasing caused by variations in the ambient magnetic field on a timescale longer than the duration between the spin-echo pulses and, with an appropriate choice of ϕ_{SE}, can compensate phase accumulation due to the presence of a static magnetic-field gradient. As they do not fundamentally affect the teleportation, we omit their effects in the following discussion.

We first prepare the state $|S\rangle_{1,3}\otimes|\downarrow\rangle_2$ in two steps: starting from the state $|\downarrow\downarrow\downarrow\rangle_{1,2,3}$ we combine the gate in equation (3) applied to ions 1 and 3 with rotations to generate[18] the state $(|\downarrow\downarrow\rangle_{1,3} - i|\uparrow\uparrow\rangle_{1,3})\otimes|\downarrow\rangle_2$, followed by implementing individual ion rotations as discussed in ref. 19 to produce $|S\rangle_{1,3}$ from $|\downarrow\downarrow\rangle_{1,3} - i|\uparrow\uparrow\rangle_{1,3}$ (see methods section). For state $|S\rangle_{1,3}\otimes|\downarrow\rangle_2$, ions 1 and 3 are in the singlet, which is invariant under a global rotation. Therefore, a global rotation $R(\theta,\phi)_{1,2,3}$ to all three ions rotates the middle ion without affecting the singlet state of ions 1 and 3, and allows us to produce the state of equation (1) for any α and β with appropriate choices of θ and ϕ.

To teleport the state of ion 2 to ion 3, we start by implementing a Bell-state measurement on Alice's qubits, ions 1 and 2. All three ions are transferred to trap 6 and then separated, with ions 1 and 2 going to trap 5 and ion 3 to trap 7. A phase gate (equation (3)) followed by a $\pi/2$-pulse, $R(\pi/2,0)$, is then applied to ions 1 and 2 in trap 5.

Our previous experiments[15] showed a significant amount of motional-mode heating during the separation process, and the separation was achieved with only a 95% success rate. Aided by a smaller separation electrode in the current trap, we can separate the ions in the desired manner with no detectable failure rate. More importantly, the heating has been significantly reduced and we find that after the separation, the stretch mode of the two ions in trap 5 is in the ground state and the centre-of-mass mode has a mean quantum number of about 1. This enables us to implement the phase gate (equation (3)) between ions 1 and 2 with fidelity greater than 90% and without the need for sympathetic recooling[12,13,17]. Ideally (and in the absence of the spin-echo pulses) this leaves the ions in the state

$$|\uparrow\uparrow\rangle_{1,2}\otimes R(\pi/2,-\pi/2)\sigma_x|\psi\rangle_3 + |\uparrow\downarrow\rangle_{1,2}\otimes R(\pi/2,-\pi/2)\sigma_y|\psi\rangle_3 + i|\downarrow\uparrow\rangle_{1,2}\otimes R(\pi/2,-\pi/2)I|\psi\rangle_3 - |\downarrow\downarrow\rangle_{1,2}\otimes R(\pi/2,-\pi/2)\sigma_z|\psi\rangle_3, \quad (4)$$

where $|\psi\rangle_3 = \alpha|\uparrow\rangle_3 + \beta|\downarrow\rangle_3$.

To complete the Bell-state measurement, we need to detect the states of ions 1 and 2 individually. We recombine all three ions in trap 6 and separate them, with ion 1 being transferred to trap 5 and ions 2 and 3 transferred to trap 7. Detection on ion 1 is then achieved through state-dependent resonance fluorescence measurements[19] ($|\downarrow\rangle$ strongly fluoresces whereas $|\uparrow\rangle$ does not), after which we optically pump the ion back to the state $|\downarrow\rangle_1$. All three ions are then recombined in trap 6 and separated again. For this separation, ions 1 and 2 are transferred to trap 5 and ion 3 is returned to trap 7. As the most recent spin-echo pulse applied in trap 6 transferred the state of ion 1 to $|\uparrow\rangle_1$, a subsequent simultaneous detection of ions 1 and 2 effectively measures the state of ion 2 with error less than 1% due to the presence of ion 1.

To complete the teleportation, we apply unitary operations to ion 3 that depend on the measurement outcomes for ions 1 and 2. We first move ions 1 and 2 to trap 2 and ion 3 to trap 5, where unitary operations consisting of a $\pi/2$-pulse, $R(\pi/2,\pi/2)$, followed by the operators σ_x, σ_y, I, σ_z for the measurement outcomes $|\uparrow\uparrow\rangle_{1,2}$, $|\uparrow\downarrow\rangle_{1,2}$, $|\downarrow\uparrow\rangle_{1,2}$, $|\downarrow\downarrow\rangle_{1,2}$ respectively, are applied. As noted above, the inclusion of the spin-echo pulses does not fundamentally change the teleportation protocol; however for $\phi_{SE} = \pi/2$, we must reorder the operations following the $\pi/2$-pulse, $R(\pi/2,\pi/2)$, to I, σ_z, σ_x, σ_y respectively. A complete experiment is about 4 ms in duration, predominantly due to three elements: the cooling of all three axial modes to the ground state (1 ms), implementing the ion separations and movements (2 ms), and the three detection durations (0.6 ms). In the future, use of smaller trap electrodes to speed up ion-separation and gate operations, coupled with better detection, should considerably increase the speed of the teleportation process.

To demonstrate the full protocol we first teleport the basis states $|\uparrow\rangle_2$ and $|\downarrow\rangle_2$, and achieve a fidelity of about 80% (78 ± 3% for $|\uparrow\rangle$ and 84 ± 2% for $|\downarrow\rangle$ for the data taken in the same run as that shown in Fig. 2). We also perform Ramsey experiments where the first $\pi/2$ pulse (having a variable phase ϕ) is applied to ion 2 (starting in the $|\downarrow\rangle_2$ state) and the second pulse (with a fixed phase) is applied to ion 3 after the teleportation is implemented. That is, $R(\pi/2,\phi)$ is applied to ion 2 and $R(\pi/2,\phi_{fixed})$ is applied to ion 3 after teleportation is completed. Ramsey fringes obtained in this way are shown in Fig. 2. We perform these experiments for $\phi_{fixed} = 0$ and $\pi/2$. From this data, we can extract the teleportation fidelities of the states $|\pm X\rangle$, $|\pm Y\rangle$, which are eigenstates of the operators σ_x and σ_y respectively. From these fidelities and those for the states $|\uparrow\rangle$ and $|\downarrow\rangle$, we determine an average fidelity $\langle F\rangle = 78 \pm 2\%$ for the teleportation process. Furthermore, if we perform the teleportation without the conditional operations, the Ramsey fringes disappear and the teleportation fidelity drops to 1/2, equivalent to Bob making a random guess for the teleported state. There are three dominant mechanisms limiting the final fidelity; imperfect preparation of the initial state $|S\rangle_{1,3}\otimes|\downarrow\rangle_2$, imperfections in the second phase gate due to heating accrued in the separation process, and dephasing of the teleported state due to fluctuating magnetic fields. We have investigated these issues in independent experiments and find that each results in a loss of 8 ± 2% in the fidelity of the final state, consistent

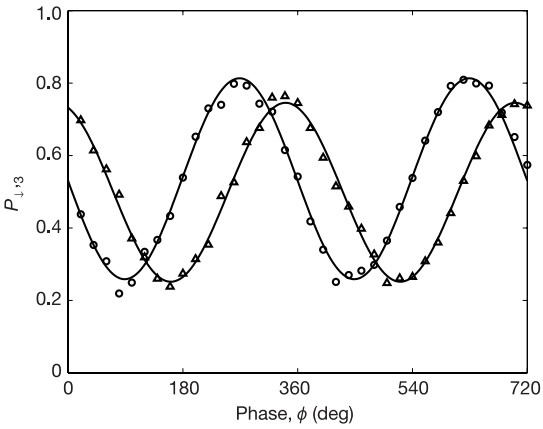

Figure 2 Ramsey fringes demonstrating the teleportation protocol. The two curves correspond to the second Ramsey pulse having $\phi_{fixed} = 0$ (circles) and $\phi_{fixed} = \pi/2$ (triangles) as discussed in the text. We plot the probability $P_{\downarrow,3}$ of observing ion 3 in the $|\downarrow\rangle_3$ state versus the phase of the first Ramsey pulse. Solid curves are best-fit sinusoidal functions to the data. The oscillations of the Ramsey fringes have an amplitude $|\rho_{\downarrow\uparrow}|$ where $\rho_{\downarrow\uparrow} = (\rho_{\uparrow\downarrow})^*$ is the off-diagonal element of the density matrix of the teleported state. The fidelity of the teleported state is then given by $F = 1/2 + |\rho_{\downarrow\uparrow}|$.

with the quoted result for teleportation. In the methods section, we discuss the effects of imperfections in the state preparation and teleportation process.

The average fidelity of 78 ± 2% achieved by our implemented quantum teleportation using atomic qubits, exceeds the value 2/3 necessary to establish the presence of entanglement[11], and is accomplished on demand and without post-selection of the data. Although teleportation has been demonstrated in other systems, our demonstration incorporates the protocol into a simple experiment in such a way that it can be viewed as a subroutine of a quantum algorithm, here, a Ramsey experiment using two separated qubits. Furthermore, our demonstration incorporates most of the important features required for large-scale quantum information processing using trapped ions[12,13]: We (a) reliably select qubits from a group and move them to separate trap zones while maintaining their entanglement, (b) manipulate and detect qubits without the need for strongly focused laser beams, and (c) perform quantum logic operations conditioned on ancilla measurement outcomes. Finally, we note that the University of Innsbruck has also implemented teleportation with the use of three Ca^+ ions in a linear Paul trap[20]. □

Methods

State preparation

Following the protocol outlined in ref. 18, three ions held in trap 5 are first laser-cooled, leaving all three axial modes in the ground state with 99% efficiency[21]. The internal states are then initialized to $|\downarrow\downarrow\downarrow\rangle$ by optical pumping. A motional phase-space 'displacement' pulse, inserted in a spin-echo sequence, is applied to the stretch mode of ions 1 and 3 by Raman beams that have a relative detuning of $\Delta\omega = \omega_s + \delta$, where ω_s is the frequency of the stretch mode and δ is a small detuning as described in ref. 18. The displacement pulse implements the transformation in equation (3) to ions 1 and 3. The spin-echo sequence acts on all three ions: a $\pi/2$-pulse, a delay T_s in which the displacement pulse acts, a π-pulse, an equal time delay T_s, and a final $\pi/2$-pulse. As the amplitude of motion for the middle ion is zero for the stretch mode, the entangling displacement pulse as described has no effect on this ion. Thus the spin-echo pulse sequence leaves the middle ion in the state $|\downarrow\rangle$, while the outer ions are affected as described in ref. 18. For an appropriate choice of detuning, δ, and pulse duration, $T = 2\pi/\delta$, we produce the state $(|\downarrow\downarrow\rangle_{1,3} - i|\uparrow\uparrow\rangle_{1,3})\otimes|\downarrow\rangle_2$ (in the experiment, $T = 9.6\,\mu s$).

To create the state $|S\rangle_{1,3}\otimes|\downarrow\rangle_2$, a second spin-echo sequence is applied with the phase of the pulses shifted by $\pi/4$ with respect to the previous sequence. In addition, for the duration of the middle π-pulse, the axial confinement is changed. The resulting change in each ion's position gives rise to a relative phase of $-\pi/4$, 0, and $+\pi/4$ for ions 1, 2 and 3, respectively[19]. For ion 2, the phase of the π-pulse is the same as the first and last $\pi/2$-pulses and the sequence leaves the ion in the state $|\downarrow\rangle_2$. The outer two ions are initially in the state $|\downarrow\downarrow\rangle_{1,3} - i|\uparrow\uparrow\rangle_{1,3}$ and the first $\pi/2$-pulse yields the state $|\downarrow\uparrow\rangle_{1,3} + |\uparrow\downarrow\rangle_{1,3}$. The π-pulse, with the $\pi/2$ phase difference on ions 1 and 3, results in the singlet state $|\uparrow\downarrow\rangle_{1,3} - |\downarrow\uparrow\rangle_{1,3}$. This state, being invariant under a global rotation, remains unchanged by the final $\pi/2$-pulse. The three-ion state is then the desired state $|S\rangle_{1,3}\otimes|\downarrow\rangle_2$. Auxiliary experiments establish a singlet fidelity $F_S = \mathrm{Tr}_2({}_{1,3}\langle S|\rho_{exp}|S\rangle_{1,3}) \approx 0.92(1)$ and a fidelity for the initial state of ion 2 of $\mathrm{Tr}_{1,3}({}_2\langle\downarrow|\rho\mathrm{exp}|\downarrow\rangle_2) \approx 0.95(1)$.

Imperfect state preparation and teleportation operations

As the operations in the experiment are imperfect, we must examine these effects to show that the observed teleportation fidelity that exceeds 2/3 could not be caused by these imperfections. In particular, as the initial state of ions 1 and 3 is not a perfect singlet, when we rotate all three qubits to prepare the state $|\psi\rangle_2 = \alpha|\uparrow\rangle_2 + \beta|\downarrow\rangle_2$, we could potentially encode this information onto bit 3 even before the teleportation process is started. We address this issue as follows: We can verify that the gate in the state preparation does not entangle bit 2 with bits 1 and 3. Therefore the most general input state is given by

$$|\Psi\rangle_{\mathrm{initial}} = (a_0|\downarrow\downarrow\rangle_{1,3} + a_1|\downarrow\uparrow\rangle_{1,3} + a_2|\uparrow\downarrow\rangle_{1,3} + a_3|\uparrow\uparrow\rangle_{1,3})\otimes(b_0|\downarrow\rangle_2 + b_1|\uparrow\rangle_2), \quad (5)$$

where, ideally, $a_1 = -a_2 = 2^{-1/2}$ and $b_0 = 1$. Here we assume that the subsequent rotation to prepare $|\psi\rangle_2$ and the teleportation operations are perfect. However, in the experiment, after preparation of $|\Psi\rangle_{\mathrm{initial}}$, we switch Raman beams from a geometry where the beams propagate at 90° to each other to a geometry where the beams co-propagate. Owing to fluctuating differences in the optical path lengths between these two sets of beams, there is a random phase difference from experiment to experiment between the corresponding Raman pulses. Over many experiments, some of the coherence terms between all three qubits average out due to this phase randomization, leading to a simplification of the calculated average fidelity with respect to the imperfections in state preparation.

The average fidelity $\langle F\rangle$ is evaluated from the expression

$$\langle F\rangle = (F(|\uparrow\rangle) + F(|\downarrow\rangle) + F(|+X\rangle) + F(|-X\rangle) + F(|+Y\rangle) + F(|-Y\rangle))/6, \quad (6)$$

where the arguments correspond to the initial state, $|\psi\rangle_2$. We find

$$\langle F\rangle = (2 - |b_0|^2)/3 + 2(2|b_0|^2 - 1)F_s/3. \quad (7)$$

When $F_s \leq 1/2$, $\langle F\rangle \leq 2/3$, and we conclude that the teleportation fidelity cannot exceed 2/3 unless the teleportation has occurred through the entangled singlet state as described in the text. Furthermore, imperfect state preparation of ion 2 contributes to an overall loss in fidelity. In a similar way, by simulation, we have also examined the effects of likely imperfections in the teleporting process and conclude that these imperfections only reduce the measured value of $\langle F\rangle$. Therefore, the experimentally measured value of $\langle F\rangle$ indicates that entanglement between bits 1 and 3 was required.

Received 17 March; accepted 4 May 2004; doi:10.1038/nature02608.

1. Bennett, C. H. *et al.* Teleporting an unknown quantum state via dual classical and Einstein-Podolsky-Rosen channels. *Phys. Rev. Lett.* **70,** 1895–1899 (1993).
2. Briegel, H.-J., Dür, W., Cirac, J. I. & Zoller, P. Quantum repeaters: The role of imperfect local operations in quantum communication. *Phys. Rev. Lett.* **81,** 5932–5935 (1998).
3. Gottesman, D. & Chuang, I. L. Demonstrating the viability of universal quantum computation using teleportation and single-qubit operations. *Nature* **402,** 390–393 (1999).
4. Bouwmeester, D. *et al.* Experimental quantum teleportation. *Nature* **390,** 575–579 (1997).
5. Furusawa, A. *et al.* Unconditional quantum teleportation. *Science* **282,** 706–709 (1998).
6. Boschi, D., Branca, S., De Martini, F., Hardy, L. & Popescu, S. Experimental realization of teleporting an unknown pure quantum state via dual classical and Einstein-Podolsky-Rosen channels. *Phys. Rev. Lett.* **80,** 1121–1125 (1998).
7. Kim, Y.-H., Kulik, S. P. & Shih, Y. Quantum teleportation of a polarization state with a complete Bell state measurement. *Phys. Rev. Lett.* **86,** 1370–1373 (2001).
8. Bowen, W. P. *et al.* Experimental investigation of continuous-variable quantum teleportation. *Phys. Rev. A.* **67,** 032302 (2003).
9. Zhang, T. C., Goh, K. W., Chou, C. W., Lodahl, P. & Kimble, H. J. Quantum teleportation of light beams. *Phys. Rev. A* **67,** 033802 (2003).
10. Nielsen, M. A., Knill, E. & Laflamme, R. Complete quantum teleportation using nuclear magnetic resonance. *Nature* **396,** 52–55 (1998).
11. Massar, M. & Popescu, S. Optimal extraction of information from finite quantum ensembles. *Phys. Rev. Lett.* **74,** 1259–1263 (1995).
12. Wineland, D. J. *et al.* Experimental issues in coherent quantum-state manipulation of trapped atomic ions. *J. Res. Natl Inst. Stand. Technol.* **103,** 259–358 (2003).
13. Kielpinski, D., Monroe, C. & Wineland, D. J. Architecture for a large-scale ion-trap quantum computer. *Nature* **417,** 709–711 (2002).
14. Nielsen, M. A. & Chuang, I. L *Quantum Computation and Quantum Information* (Cambridge Univ. Press, Cambridge, 2000).
15. Rowe, M. A. *et al.* Transport of quantum states and separation of ions in a dual rf ion trap. *Quant. Inf. Comp.* **2,** 257–271 (2002).
16. Wineland, D. J. *et al.* Quantum information processing with trapped ions. *Phil. Trans. R. Soc. Lond. A* **361,** 1349–1361 (2003).
17. Barrett, M. D. *et al.* Sympathetic cooling of $^9Be^+$ and $^{24}Mg^+$ for quantum logic. *Phys. Rev. A* **68,** 042302 (2003).
18. Leibfried, D. *et al.* Experimental demonstration of a robust, high-fidelity geometric two ion-qubit phase gate. *Nature* **422,** 412–415 (2003).
19. Rowe, M. A. *et al.* Experimental violation of a Bell's inequality with efficient detection. *Nature* **409,** 791–794 (2001).
20. Riebe, M. *et al.* Deterministic quantum teleportation with atoms. *Nature* (this issue).
21. King, B. E. *et al.* Cooling the collective motion of trapped ions to initialize a quantum register. *Phys. Rev. Lett.* **81,** 1525–1528 (1998).

Acknowledgements This work was supported by ARDA/NSA and NIST. We thank J. Bollinger and J. Martinis for helpful comments on the manuscript. T.S. acknowledges a Deutsche Forschungsgemeinschaft research grant. This paper is a contribution of the National Institute of Standards and Technology and is not subject to US copyright.

Competing interests statement The authors declare that they have no competing financial interests.

Correspondence and requests for materials should be addressed to D.J.W. (djw@boulder.nist.gov)

In situ observation of colloidal monolayer nucleation driven by an alternating electric field

Ke-Qin Zhang & Xiang Y. Liu

Department of Physics, National University of Singapore, 2 Science Drive 3, Singapore 117542

The nucleation of crystalline materials is a hotly debated subject in the physical sciences[1]. Despite the emergence of several theories in recent decades[2–7], much confusion still surrounds the dynamic processes of nucleation[5–7]. This has been due in part to the limitations of existing experimental evidence. Charged